Supplement material

for

An octanuclear 3-phenyl-5-(2-pyridyl)pyrazolate/phenylsilsesquioxane complex: synthesis, unique structure, and catalytic activity

by

Alexey N. Bilyachenko, Victor N. Khrustalev, Zhibin Huang, Lidia S. Shul'pina, Pavel V. Dorovatovskii, Elena S. Shubina, Nikolay S. Ikonnikov, Nikolai N. Lobanov, Karim Ragimov, and Di Sun

General Experimental Considerations

3-(5-phenyl-1H-pyrazol-3-yl)pyridine and 2-methyl-5-(5-phenyl-1H-pyrazol-3-yl)pyridine have been prepared according approach published earlier.[s1] All other reagents were purchased from the usual suppliers (Sigma, Fluka) and used without further purification. Elemental analyses were carried out with an XRF spectrometer VRA-30. IR spectra of the compounds (KBr pellets) were measured on a Shimadzu IR Prestige 21 FT-IR Spectrophotometer equipped with an MCT detector using a Miracle single reflection ATR unit by Pike. Set of signals: 1410–1370 cm^{-1} (νstretchC–Si), 1110 cm^{-1} (νasSi–O–Si), 1040 cm^{-1} (νsSi–O–Si), 950 cm^{-1} (νasSi–O in Si–O–M fragment), 820 cm^{-1} and 760 cm^{-1} (νwagC–Si).

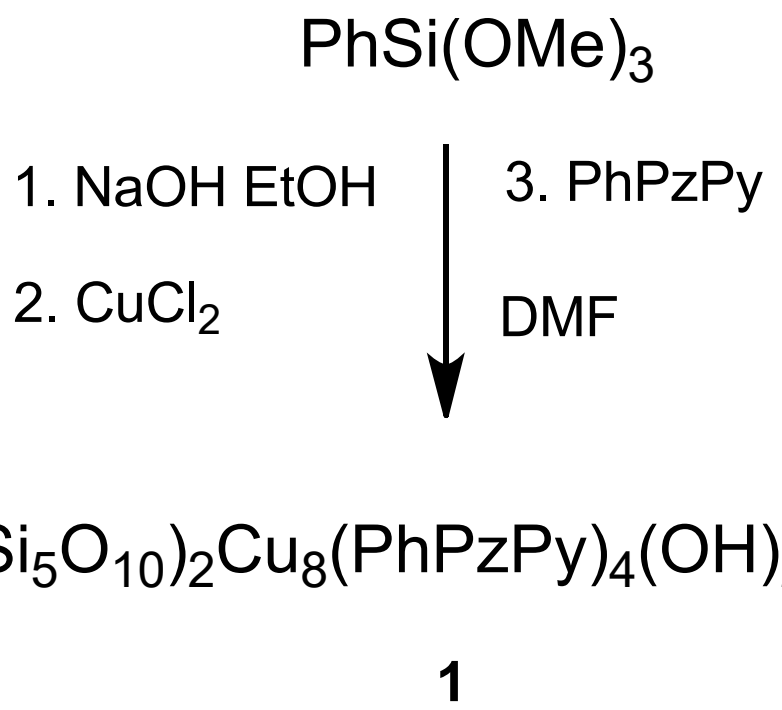

Scheme S1. Synthesis of octacopper 3-phenyl-5-(2-pyridyl)pyrazolate/phenyl-silsesquioxane complex **1**.

Synthesis of **1**.

0.50 g (2.53 mmol) of $PhSi(OMe)_3$ and 0.16 g (4 mmol) of NaOH were heated at reflux in 30 mL of ethanol for 2 h. Then, 0.27 g (2 mmol) of $CuCl_2$ was added, and the resulting mixture was stirred without heating for 48 h. Afterwards, 0.22 g (1 mmol) of 3-phenyl-5-(2-pyridyl)pyrazole was added and the resulting mixture was heated at reflux for 1 h and then stirred without heating overnight followed by the centrifugation of precipitate. Crystallization of filtrate, which was mixed with 15 ml of DMF, gave in a week a crystalline material, including single crystals that were used for X-ray diffraction and XRD analyses. Powder pattern was measured on a Tongda TDM-20 diffractometer at room temperature (CuKα radiation, Ni filter, θ/2θ scan from 4° to 40°). The remaining part of the crystalline material was dried in vacuum to calculate yield.

Anal. Calcd for $[(Ph_5Si_5O_{10})_2Cu_8(PhPzPy)_4(OH)_2]$: Cu, 18.19; N, 6.01; Si, 10.05. Found: Cu, 18.10; N, 5.90; Si, 9.95. Yield: 0.53 g (76%).

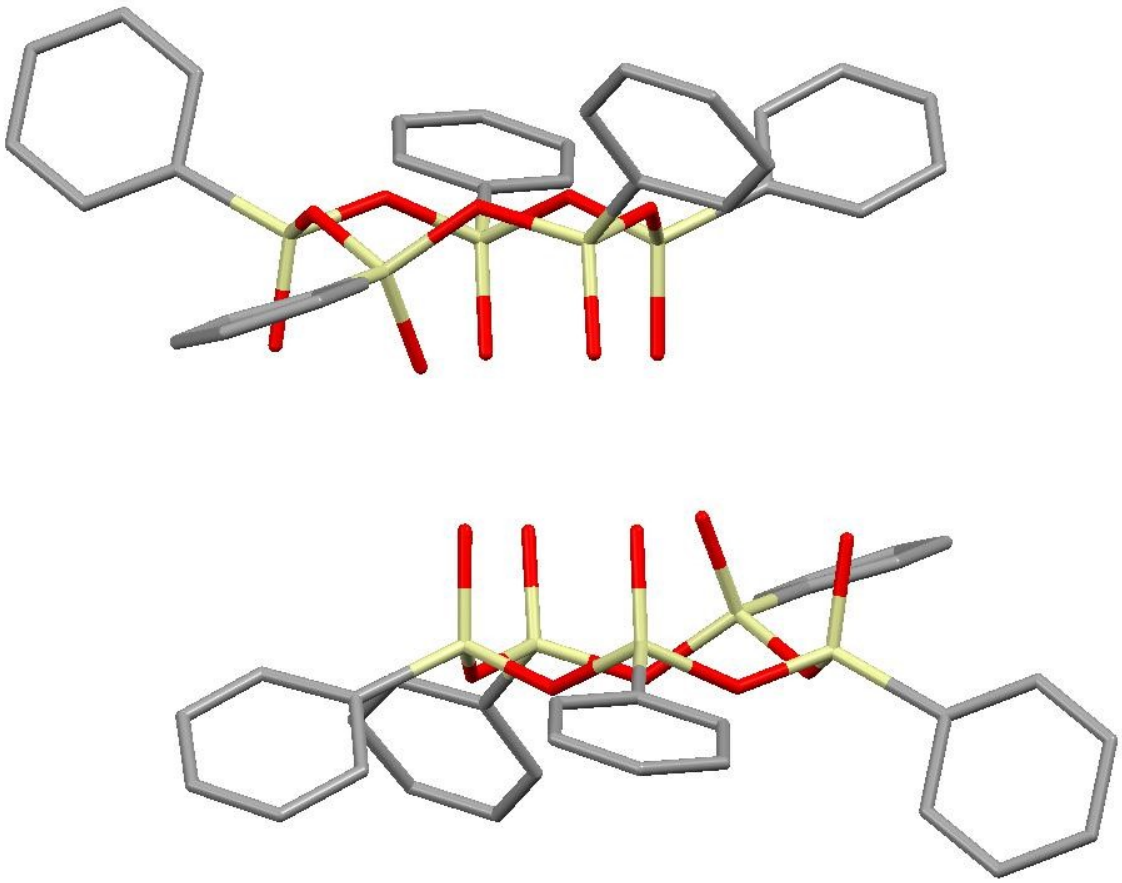

Figure S1. Structure of silsesquioxane ligands in complex **1**. Hydrogen atoms are omitted for clarity.

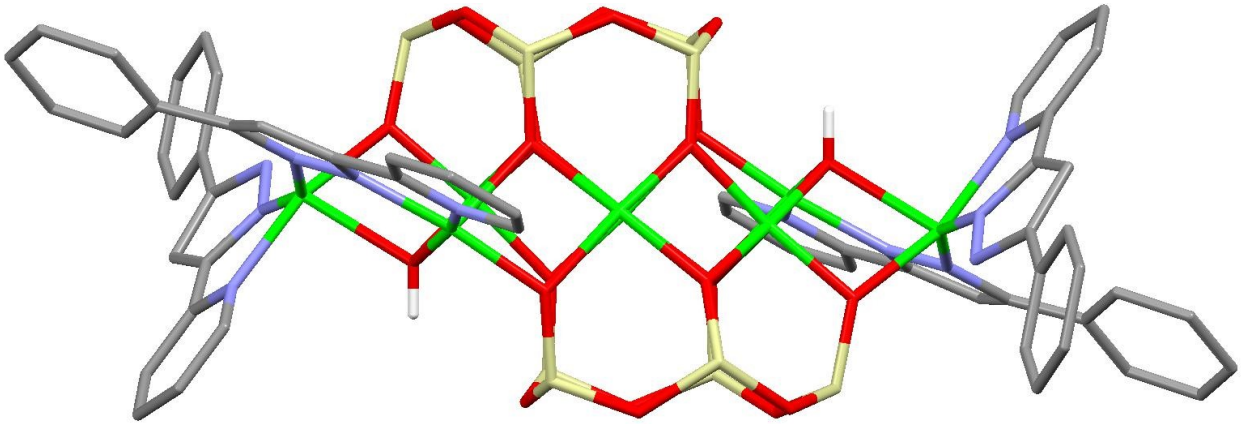

Figure S2. Side view of complex **1**. DMF molecules, phenyl groups at silicon atoms and hydrogen atoms (except for charge balancing OH groups) are omitted for clarity.

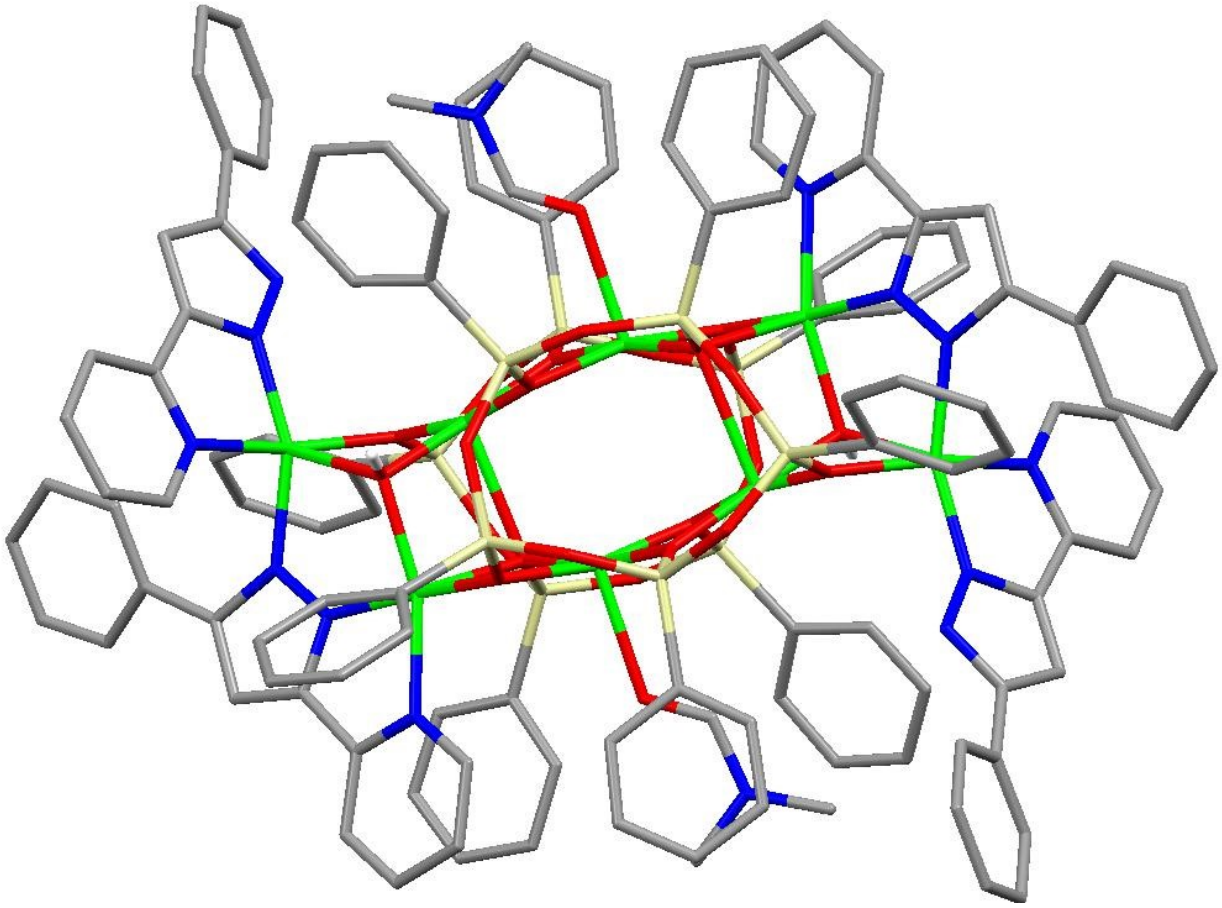

Figure S3. Top view of complex **1**.

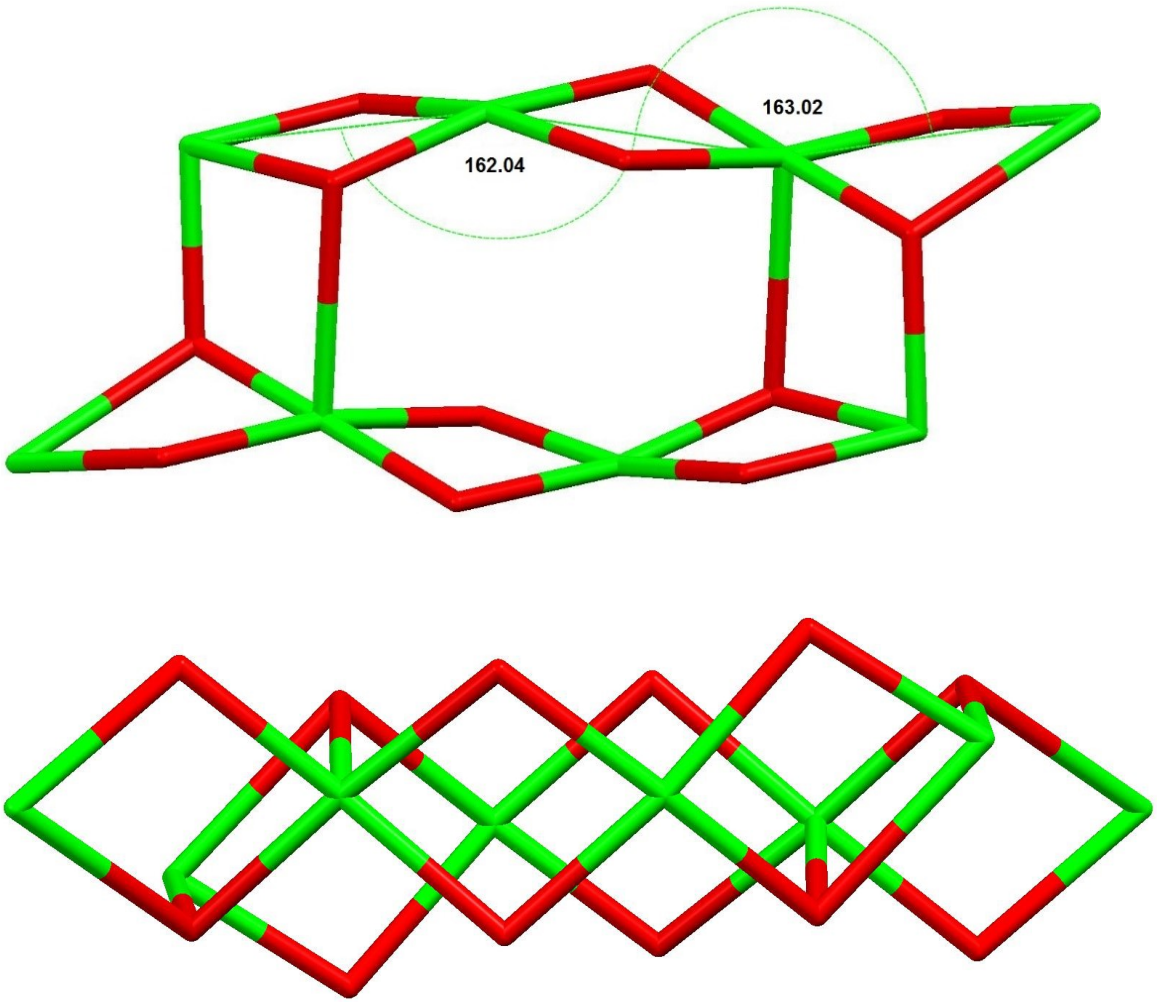

Figure S4. Two projections of metal oxide fragment in complex **1**. Upper projection shows *zigzag*-like structure of copper tetramers.

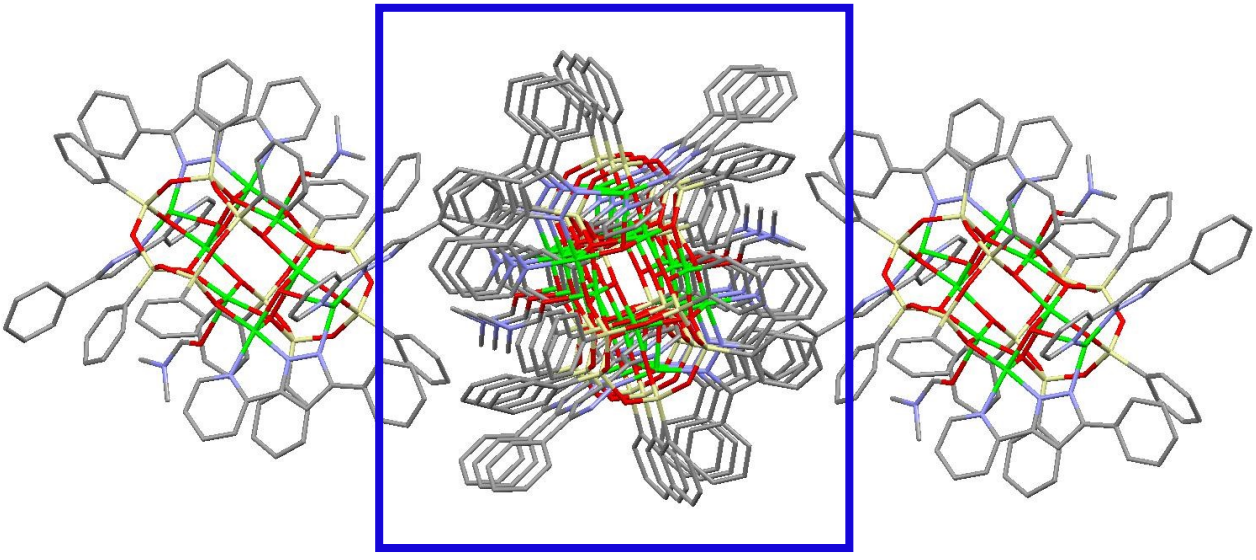

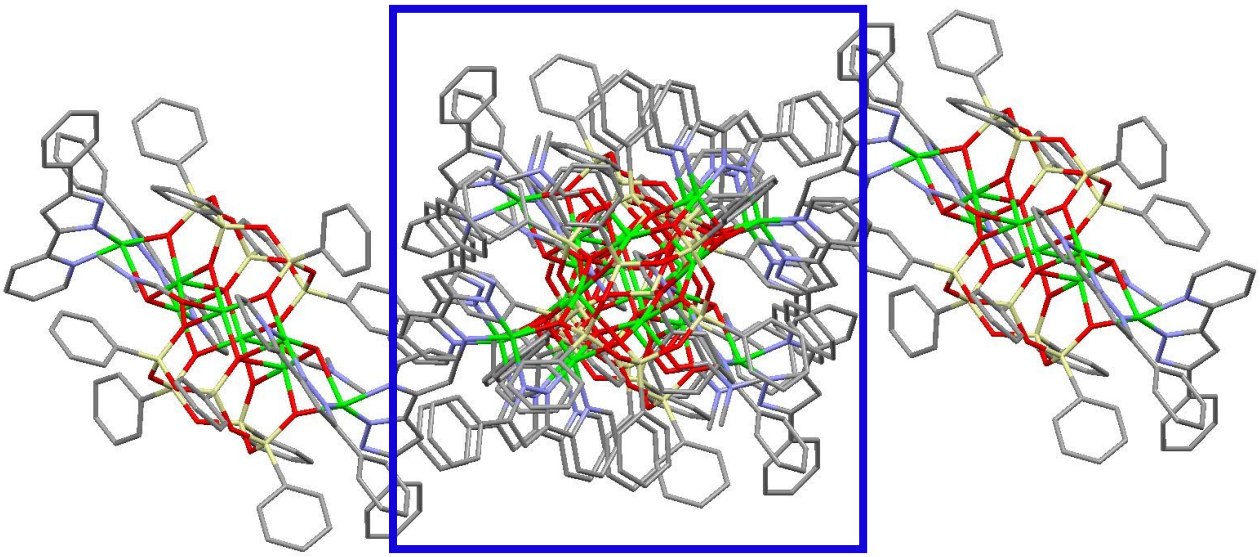

Figure S5. Two perpendicular projections of crystal packing of complex **1**. Upper projection shows the same orientation of central cages, giving an overlay. Lower projection shows the rotation of central cages, giving an absence of an overlay

Figure S6 shows powder patterns of complex **1**. Experimental (a) pattern (measured at room temperature) and calculated ones (from single crystal X-ray diffraction data obtained at 100 K) correspond well to each other. Small shifts of several peaks and redistribution of intensities point at some changes of cell parameters of polycrystalline sample in comparison to those of single crystal sample which could be attributed to a difference of temperatures (298 K vs 100K).

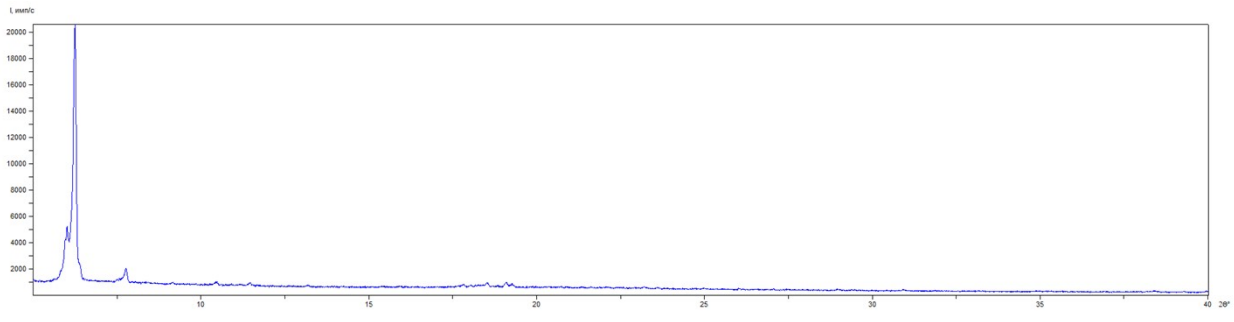

a

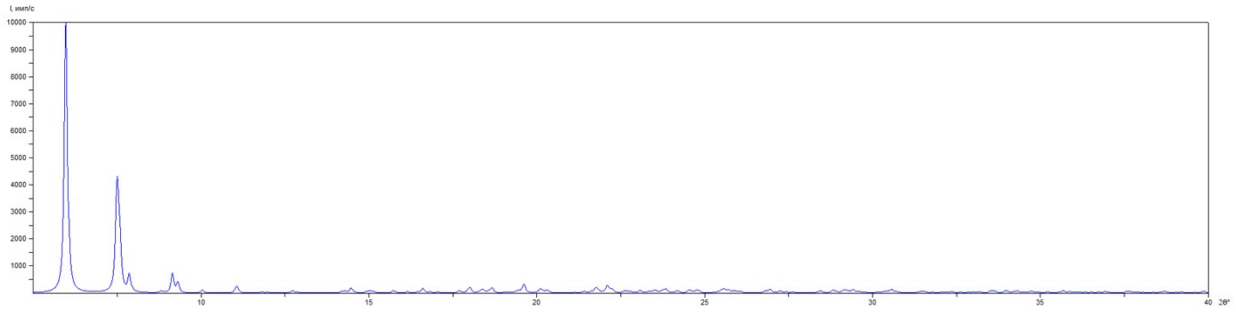

b

Figure S6. Powder patterns of sample **1**: experimental (top, a) and calculated (bottom, b).

Further studies allowed us to expand a list of PyPz-ligands, applicable for the synthesis of compound **1**' analogs. Namely, self-assembly reaction including 2-methyl-5-(5-phenyl-1H-pyrazol-3-yl)pyridine (Scheme S2) smoothly gave complex $[(Ph_5Si_5O_{10})^{5-}{}_2Cu^{2+}{}_8(PhPzPy\text{-}Me)^{1-}{}_4(OH)^{1-}{}_2]$ **1a** in 70% yield. Complex **1a** is predictably very similar by its structure to compound **1** (Figure S7). Tetrameric Cu…Cu…Cu…Cu fragments in **1a** are more linear than in case of complex **1** (163.47° and 171.58° vs 162.04 and 163.02, respectively). Most probably, this is due to an absence of coordinated solvate molecules in composition of complex **1a**. The longest intramolecular Cu…Cu distance in **1a** (10.951 Å) is shorter than in case of **1** (11.075 Å).

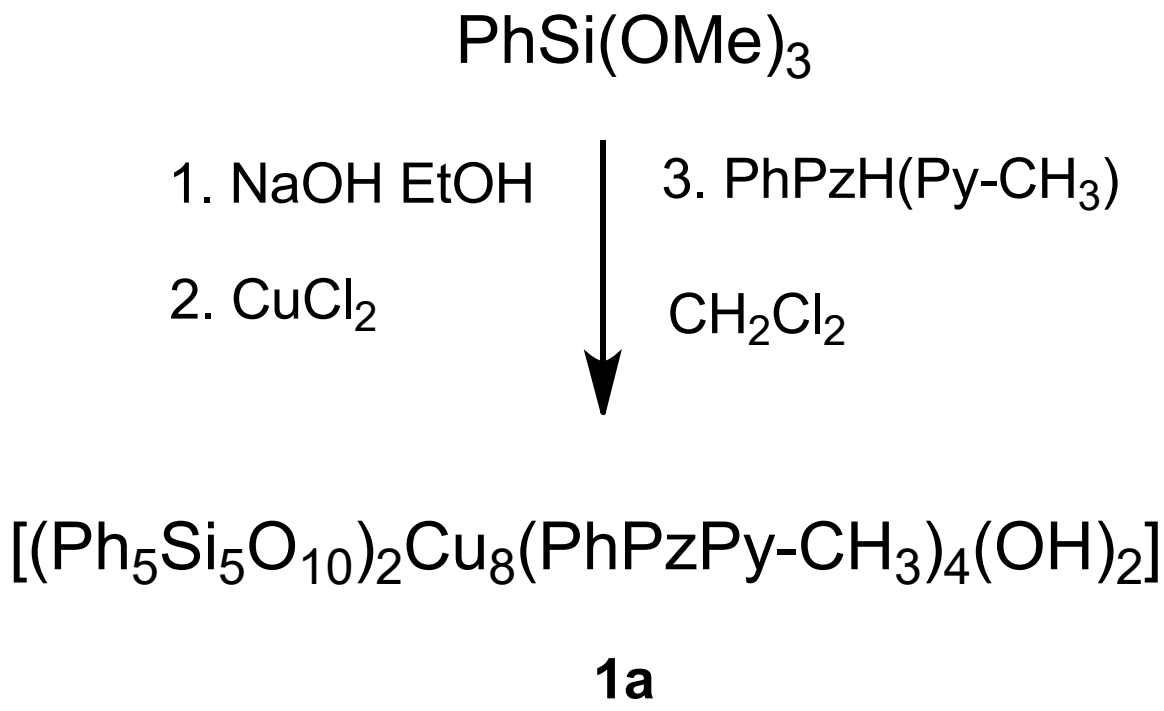

Scheme S2. Synthesis of octacopper 2-methyl-5-(5-phenyl-1H-pyrazol-3-yl)pyridine/phenylsilsesquioxane complex **1a**.

Synthesis of **1a**.

0.50 g (2.53 mmol) of $PhSi(OMe)_3$ and 0.16 g (4 mmol) of NaOH were heated at reflux in 30 mL of ethanol for 2 h. Then, 0.27 g (2 mmol) of $CuCl_2$ was added, and the resulting mixture was stirred without heating for 48 h. Afterwards, 0.24 g (1 mmol) of 2-methyl-5-(5-phenyl-1H-pyrazol-3-yl)pyridine was added and the resulting mixture was heated at reflux for 1 h and then stirred without heating overnight followed by the centrifugation of precipitate. Crystallization of filtrate, which was mixed with 15 ml of CH_2Cl_2, gave in a week a crystalline material, including single crystals that were used for X-ray diffraction. The remaining part of the crystalline material was dried in vacuum to calculate yield.

Anal. Calcd for $[(Ph_5Si_5O_{10})_2Cu_8(PhPzPy\text{-}Me)_4(OH)_2]$: Cu, 17.83; N, 5.89; Si, 9.85. Found: Cu, 17.76; N, 5.82; Si, 9.79. Yield: 0.50 g (70%).

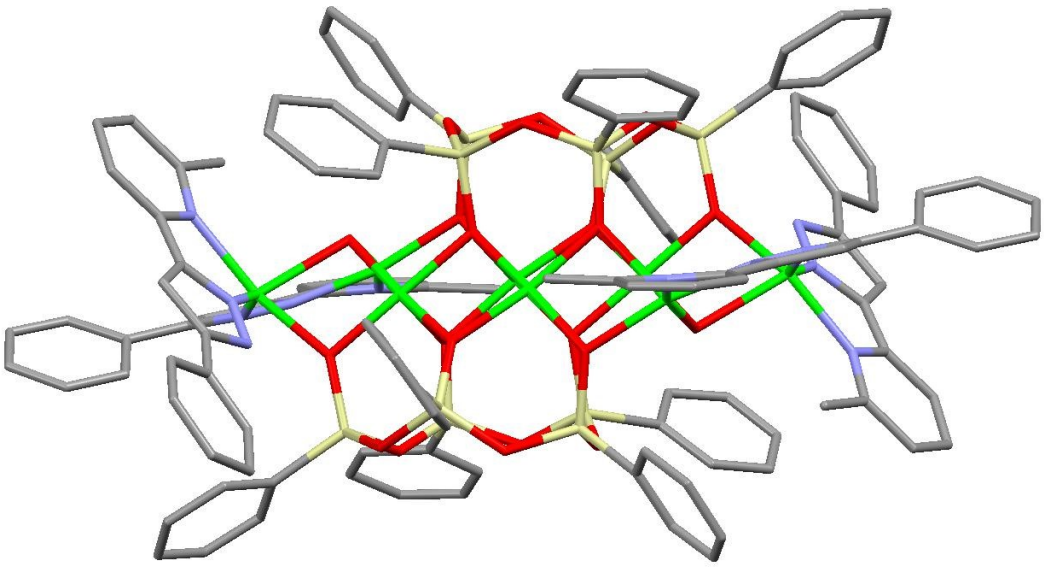

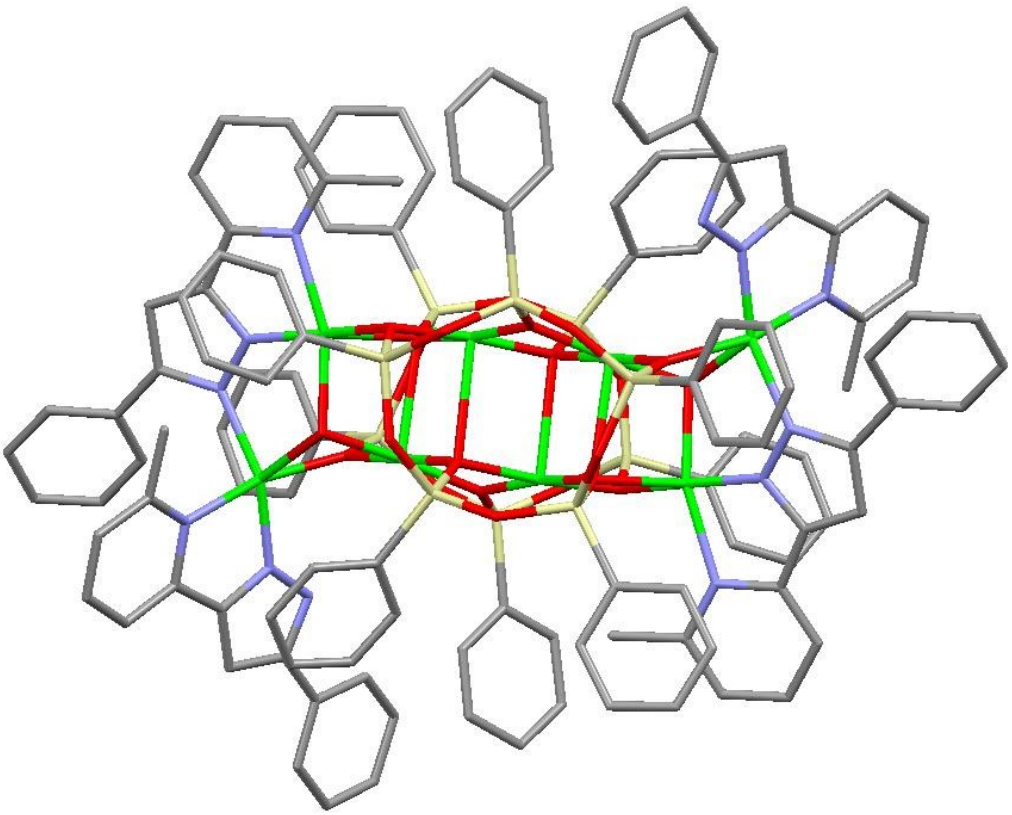

Figure S7. Two projections of complex **1a**. Hydrogen atoms are omitted for clarity.

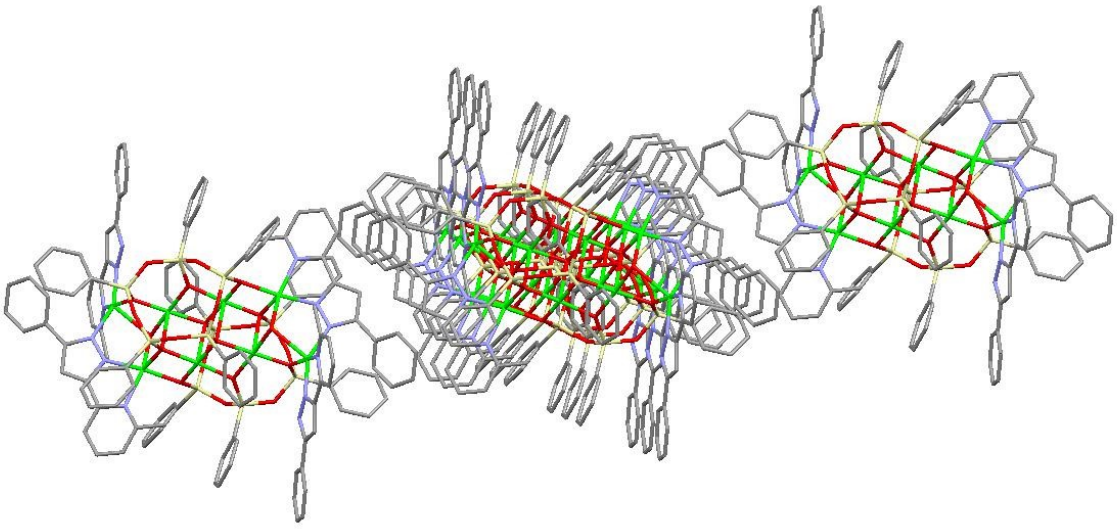

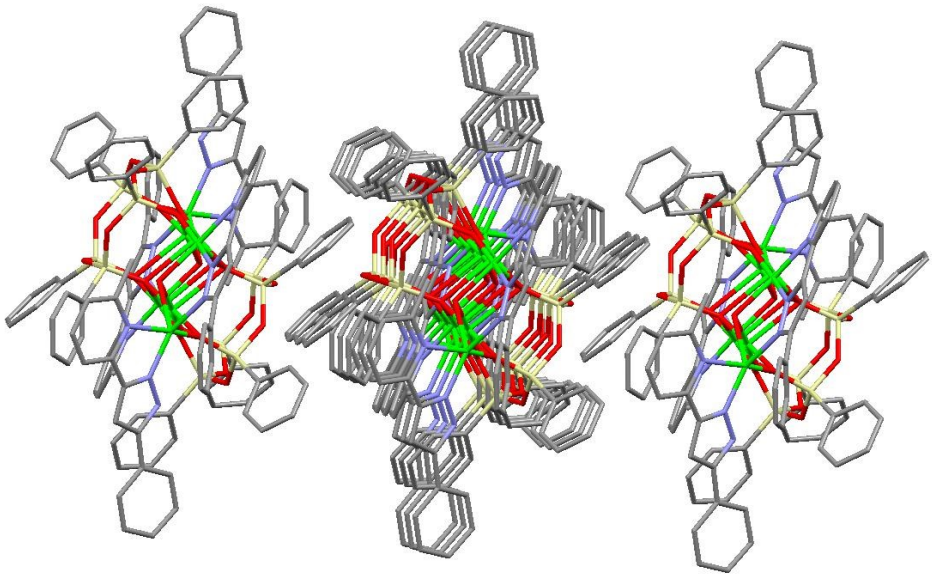

Figure S8. Two perpendicular projections of crystal packing of complex **1a**, showing an absence of rotated cages (overlays are seen in both directions).

In turn, synthesis of **1** is reproducible and smoothly provided a close analog of complex **1**, namely compound **1b** of $[(Ph_5Si_5O_{10})^-{}_2Cu_8(PhPzPy)_4(OH)_2(DMF)_2]$ 2DMF composition. The only difference between two these compounds is a presence of two non-coordinated DMF molecules in the composition of **1b.** The main structural feature of complexes **1**-**1b** is a presence of deprotonated PyPz ligands. It was of interest to investigate other types of auxiliary organic ligands, capable to act in a similar manner. In this line of thought, self-assembly synthesis of coppersilsesquioxane complex with 8-hydroxyquinoline has been performed (Scheme S3). Ratio of reactants was oriented on composition of complex **1** (10Si:8Cu:4 hydroxyquinolates). According to expectations, close analog of complex **1**, complex $[(Ph_5Si_5O_{10})_2Cu_8(hq)_4(OH)_2]$ **2** has been isolated in 69% yield.

Synthesis of **2**.

0.50 g (2.53 mmol) of $PhSi(OMe)_3$ and 0.16 g (4 mmol) of NaOH were heated at reflux in 30 mL of ethanol for 2 h. Then, 0.27 g (2 mmol) of $CuCl_2$ was added, and the resulting mixture was stirred without heating for 48 h. Afterwards, 0.22 g (1 mmol) of 8-hydroxyquinoline was added and the resulting mixture was heated at reflux for 1 h and then stirred without heating overnight followed by the centrifugation of precipitate. Crystallization of filtrate, which was mixed with 15 ml of DMF, gave in a 4-5 days a crystalline material, including single crystals that were used for X-ray diffraction analysis. The remaining part of the crystalline material was dried in vacuum to calculate yield.

Anal. Calcd for $[(Ph_5Si_5O_{10})_2Cu_8(hq)_4(OH)_2]$: Cu, 20.41; N, 2.25; Si, 11.28. Found: Cu, 20.32; N, 2.19; Si, 11.90. Yield: 0.43 g (69%).

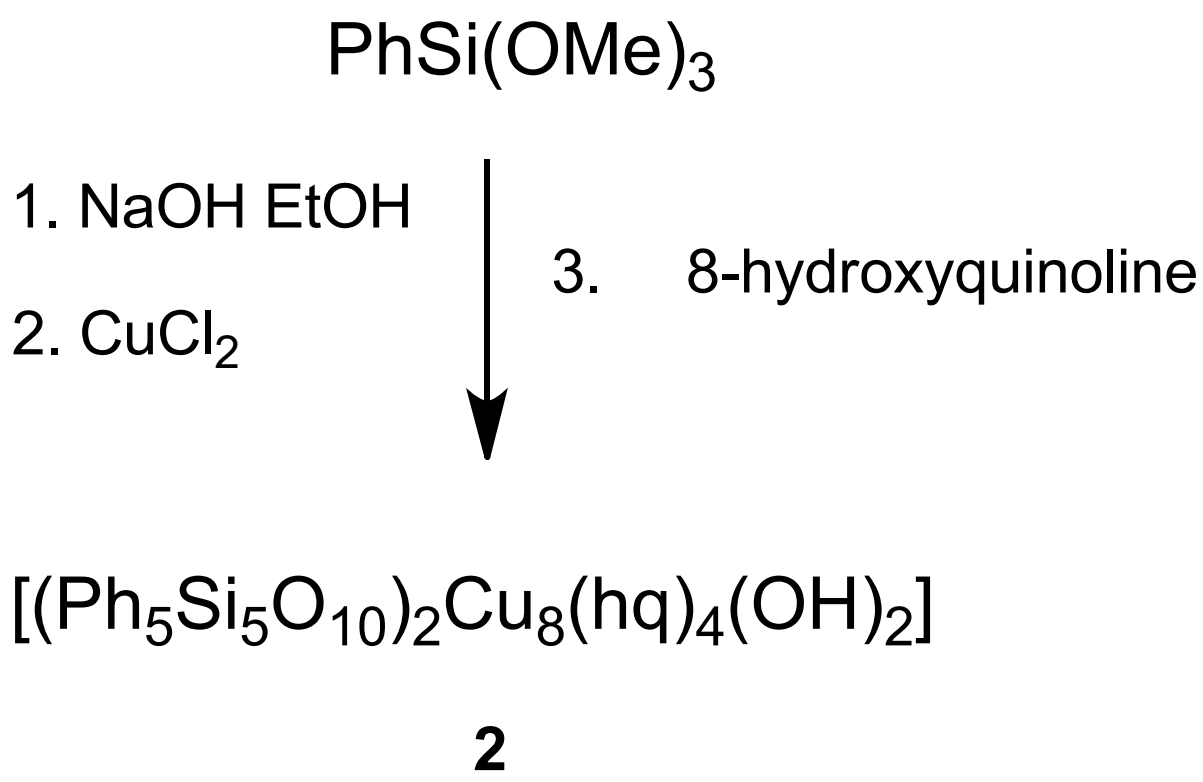

Scheme S3. Synthesis of octacopper 8-hydroxyquinolate/phenylsilsesquioxane complex **2**.

Compound **2** shows significant similarity to complex **1** (Figures S9-S10). First of all, it concerns different behaviors of 8-hydroxyquinolate ligands. Two of hydroxyquinolates act as bridging ligands, while other two – only as chelating ones. In turn, one could see some differences, provoking by the change of organic ligands in complexes **1-1a** and **2**. Tetrameric Cu…Cu…Cu…Cu fragments in **2** are much more linear than in case of complex 1 (Figure S11). Most probably, this is due to an absence of coordinated solvate molecules in composition of complex **2**. The longest intramolecular Cu…Cu distance in **2** (10.875 Å) is shorter than in case of **1-1a** (11.075 Å and 10.951 Å, respectively). Finally, packing of complex **2** represents an alternation of rotated cages (Figure S11).

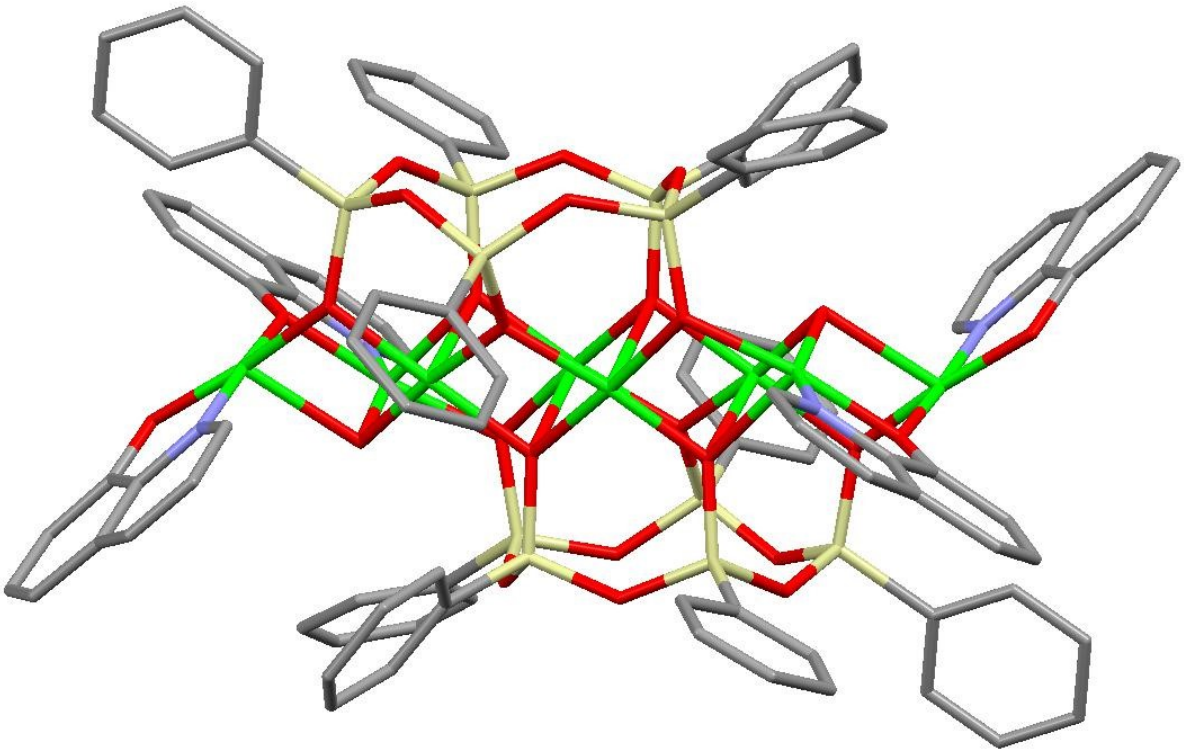

Figure S8. Side view of complex **2**. Hydrogen atoms are omitted for clarity.

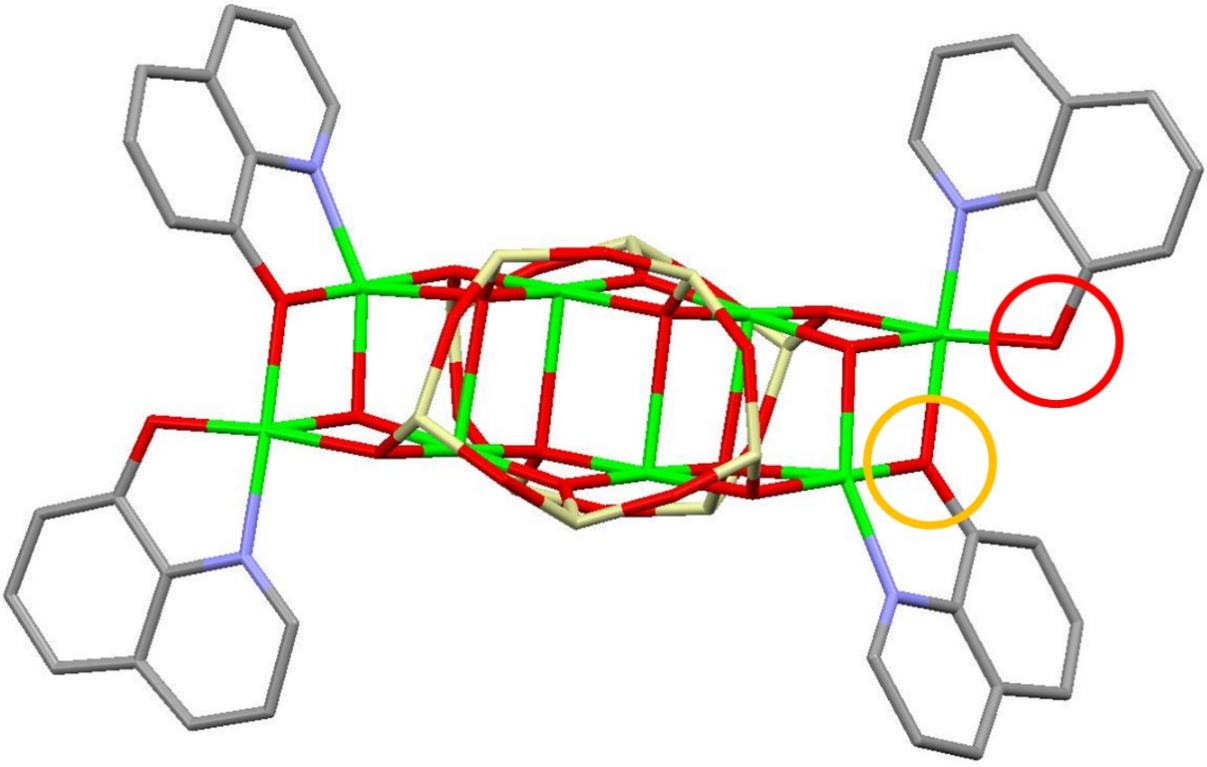

Figure S9. Top view of complex **2**. Phenyl groups at silicon atoms and hydrogen atoms are omitted for clarity. Circles are to represent bridging (orange circle) and chelating (red circle) ligation styles of 8-hydroxyquinolate fragments.

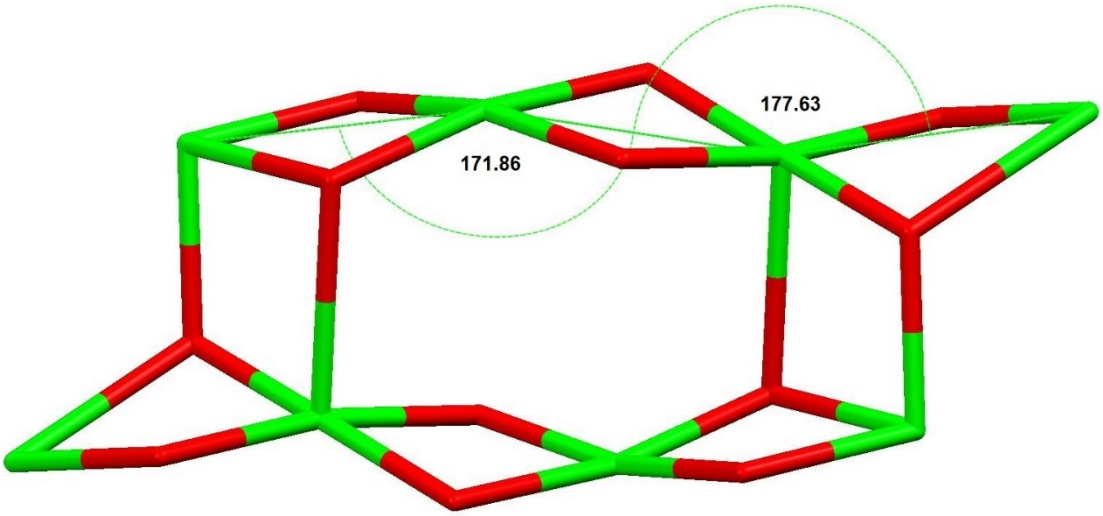

Figure S10. Metal oxide fragment in complex **2**.

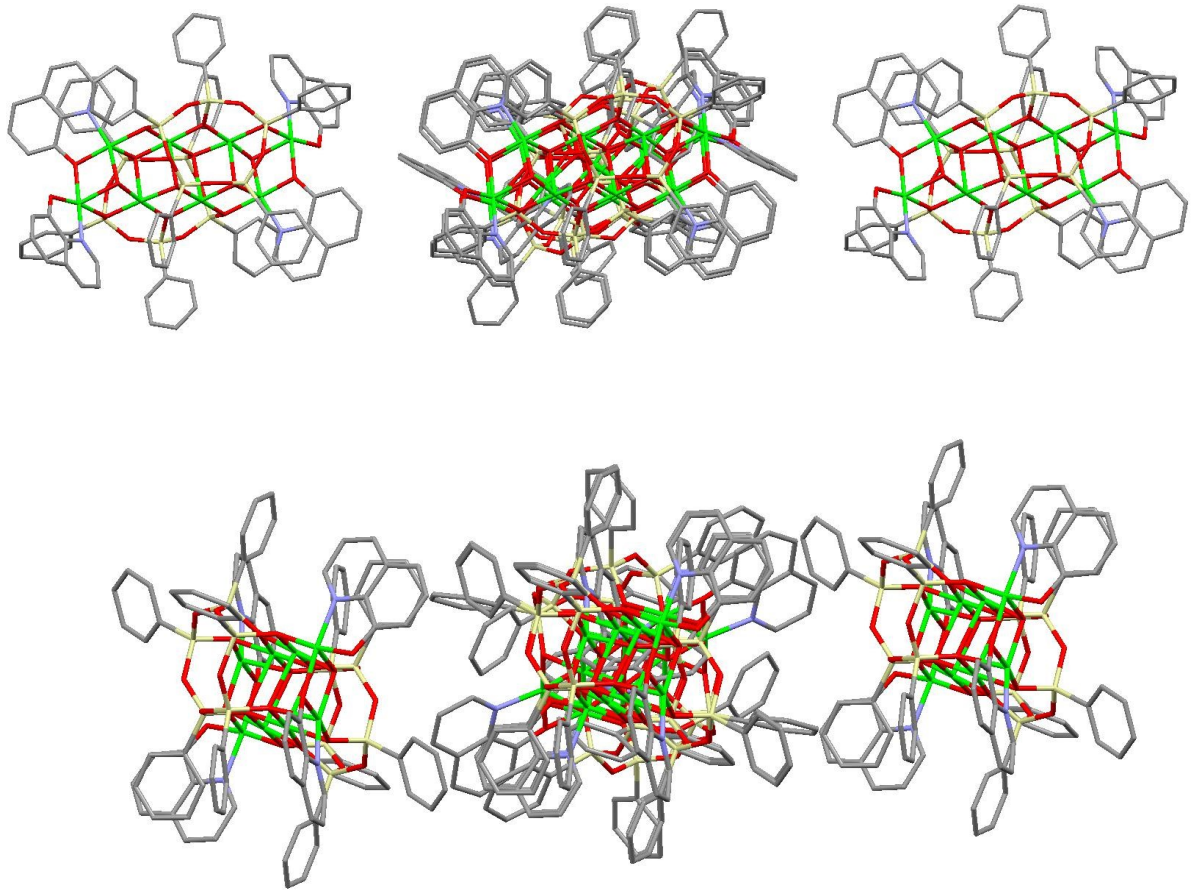

Figure S11. Two perpendicular projections of crystal packing of complex **2**, showing a presence of rotated cages (overlays are not seen in both directions).

X-ray crystal structure determination

The single-crystal X-ray diffraction data for **1** and **2** were collected on the 'Belok/RSA' beamline of the National Research Center 'Kurchatov Institute' (Moscow, Russian Federation) using a Rayonix SX165 CCD detector. In total, 720 frames were collected with an oscillation range of 1.0° in the φ scanning mode using two different orientations for each crystal. The data were indexed and integrated by the utility *iMOSFLM* in CCP4 program [S2] and corrected for absorption using the *Scala* program [S3]. The single-crystal X-ray diffraction study of **1a** was carried out on a four-circle Rigaku Synergy-S diffractometer equipped with a HyPix6000HE area-detector (T = 100 K, graphite monochromator, shutterless ω-scanning mode). The data were integrated and corrected for absorption by the *CrysAlisPro* program [S4]. For details, see Table S1.

The structures were solved by direct methods and refined by a full-matrix least squares technique on F^2 with anisotropic displacement parameters for non-hydrogen atoms. All attempts to model and refine positions of the strongly disordered solvate ethanol (in **1**), methylenechloride (in **1a**) and dimethylformamide (in **1b** and **2**) molecules were unsuccessful. Therefore, their contribution to the total scattering pattern was removed by use of the utility *SQUEEZE* in PLATON15 [S5]. The hydrogen atoms of the hydroxyl groups were localized in the difference-Fourier maps and refined within riding model with fixed isotropic displacement parameters [U_{iso}(H) = 1.5U_{eq}(O)]. The other hydrogen atoms were placed in calculated positions and included in the refinement within riding model with fixed isotropic displacement parameters [U_{iso}(H) = 1.5U_{eq}(C) for the CH_3-groups and 1.2U_{eq}(C) for the other groups]. All calculations were carried out using the SHELXTL program [S6].

Crystallographic data have been deposited with the Cambridge Crystallographic Data Center, CCDC 2375632 (**1**), CCDC 2381999 (**1a**) CCDC 2390608 (**1b**) and CCDC 2375633 (**2**). Copies of this information may be obtained free of charge from the Director, CCDC, 12 Union Road, Cambridge CB2 1EZ, UK (Fax: +44 1223 336033; e-mail: deposit@ccdc.cam.ac.uk or www.ccdc.cam.ac.uk).

Table 1. Crystal data and structure refinement for the compounds studied.

Identification code	**1**	**1a**	**1b**	**2**
Empirical formula	$C_{122}H_{106}Cu_8N_{14}O_{24}Si_{10}$	$C_{120}H_{100}Cu_8N_{12}O_{22}Si_{10}$	$C_{128}H_{120}Cu_8N_{16}O_{26}Si_{10}$	$C_{96}H_{76}Cu_8N_4O_{26}Si_{10}$
Formula weight	2941.52	2851.43	3087.71	2490.91
Crystal size, mm	0.03 × 0.06 × 0.09	0.09 × 0.12 × 0.13	0.13 × 0.17 × 0.22	0.03 × 0.06 × 0.09
Wavelength, Å	0.75270	1.54184	1.54184	0.74500
Crystal system	Monoclinic	Triclinic	Triclinic	Monoclinic
Space group	$P2_1/n$	P-1	P-1	$P2_1/c$
a, Å	15.6459(12)	12.3924(2)	19.0322(3)	17.8329(16)
b, Å	18.9911(14)	17.2730(3)	19.1168(3)	16.5280(15)
c, Å	24.7090(19)	17.8005(3)	19.7780(2)	20.4641(19)
α, deg.	90	64.6067(17)	89.5344(10)	90
β, deg.	107.086(3)	89.6243(14)	87.6687(10)	106.432(11)
γ, deg.	90	79.3532(14)	71.8144(12)	90
V, Å^3	7017.8(9)	3371.53(11)	6830.75(17)	5785.3(10)
Z	2	1	2	2
Density (calc.), g/cm^3	1.392	1.404	1.501	1.430
μ, mm^{-1}	1.566	2.761	2.803	1.830
F(000)	3000	1452	3160	2520
Theta range, deg.	2.151 – 27.000	2.891 – 79.939	2.236 – 80.279	2.530 – 31.002
Index ranges	$-18 \le h \le 18$, $-20 \le k \le 22$, $-29 \le l \le 29$	$-15 \le h \le 15$, $-21 \le k \le 18$, $-22 \le l \le 22$	$-24 \le h \le 24$, $-24 \le k \le 24$, $-25 \le l \le 24$	$-24 \le h \le 24$, $-22 \le k \le 22$, $-25 \le l \le 28$
Reflections collected	40179	85875	112915	86211
Independent reflections, R_{int}	12379, 0.0626	14369, 0.0683	28936, 0.0586	15724, 0.0687
Reflections observed	10171	12926	24569	8805
R_1 / wR_2 ($I > 2\sigma(I)$)	0.1370 / 0.2895	0.1178 / 0.2716	0.0593 / 0.1554	0.0761 / 0.1819
R_1 / wR_2 (all data)	0.1537 / 0.2984	0.1233 / 0.2738	0.0697 / 0.1633	0.1320 / 0.2159
Goodness-of-fit on F^2	1.032	1.025	1.023	1.072
Extinction coefficient	0.0031(3)	–	–	0.0042(4)
T_{min} / T_{max}	0.888 / 0.945	0.793 / 1.000	0.684 / 1.000	0.844 / 0.936
$\Delta\rho_{max}$ / $\Delta\rho_{min}$, e·Å^{-3}	1.888 / -1.079	2.231 / -1.054	1.535 / -1.163	0.592 / -1.308

Complex 1 as a catalyst in oxidations with peroxides

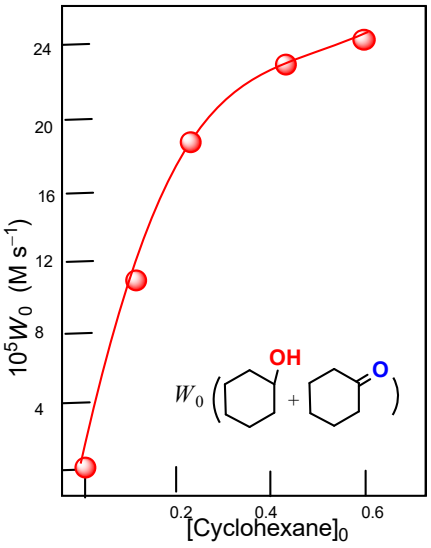

Figure S12. Dependence of the initial rate of oxygenates formation W_0 on initial concentration of cyclohexane in oxidation of cyclohexane with hydrogen peroxide (2.0 M, 50 % aqueous, 0.32ml) catalyzed by compound **1** (5×10^{-4}M, 3mg) in MeCN (up to 2.5ml) at 50 °C. Concentrations of cyclohexanone and cyclohexanol were determined after reduction of the aliquots with solid PPh_3.

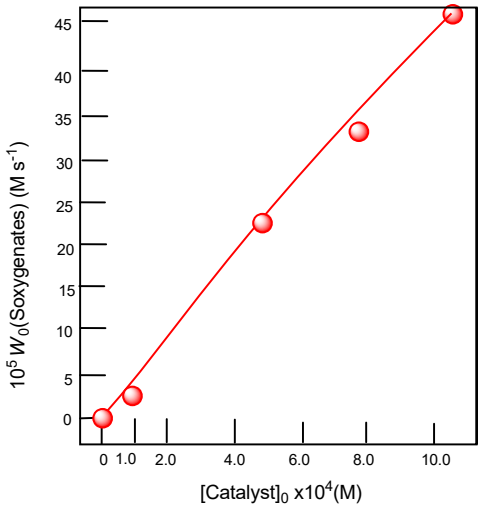

Figure S13. Dependence of the initial rate of oxygenate (sum cyclohexanol+cyclohexanone) formation W_0 in the oxidation of cyclohexane (0.46M) with hydrogen peroxide (2.0 M, 50 % aqueous) catalyzed by compound **1** in MeCN up to 2.5ml, at 50° C on the initial concentration of catalyst

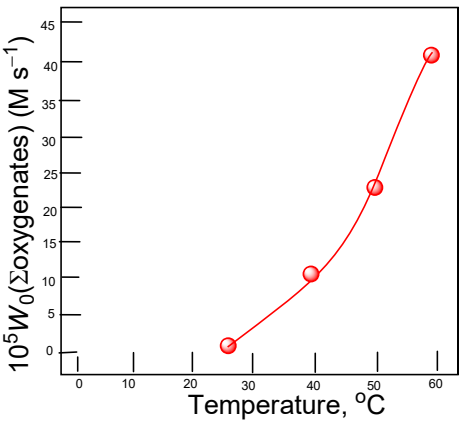

Figure S14. Dependence of the initial rate of oxygenate (sum cyclohexanol+cyclohexanone) formation W_0 in the oxidation of cyclohexane (0.46M) with hydrogen peroxide (2.0 M, 50 % aqueous) catalyzed by compound **1** (5×10^{-4} M) in MeCN up to 2.5ml on reaction temperature

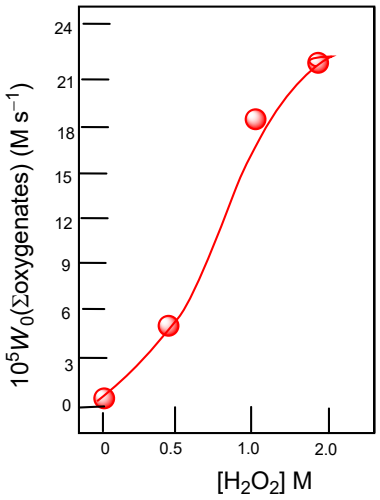

Figure S15. Dependence of the initial rate of oxygenate (sum cyclohexanol+cyclohexanone) formation W_0 in the oxidation of cyclohexane (0.46M) with hydrogen peroxide catalyzed by compound **1** (5×10^{-4} M) in MeCN up to 2.5ml on concentration of hydrogen peroxide

We determined the selectivity parameters for the oxidation of certain alkanes: *n*-heptane and methylcyclohexane) by hydrogen peroxide catalyzed by complex **1**. For *n*-heptane, after two hours, the following concentrations of (M) alcohol isomers were obtained (after reduction with triphenylphosphine): C (1) 0.005M; C (2) 0.02M; C (3) 0.02M; C (4) 0.01M (the yield 14%). These values gave a series of selectivity: C (1): C (2): C (3): C (4) = 1.0: 6.0: 6.0: 6.0. In the case of methylcyclohexane oxidation (yield 15%) the following selectivity parameters were obtained: 1°: 2°: 3° = 1.0: 5.5: 14.9. The selectivity parameters measured in the oxidation alkanes are close to the parameters typical for the reactions of alkanes with hydroxyl radicals.[53-55]

Experimental part

Oxidation of alkanes and alcohols

Pyrex cylindrical vessels with vigorous stirring of the oxidation reaction mixture were typically carried out in air in thermostated solution (**CAUTION**: the combination of air or molecular oxygen and H_2O_2 with organic compounds at elevated temperatures may be explosive!). Initially, a portion (0.32 ml, 2M) of 50% aqueous solution of hydrogen peroxide (for alkanes) or a portion (0.36ml, 1.5M) of 70% aqueous solution of *tert*-butylhydroperoxide (for alcohols) were added to the solution of the catalyst ($5x10^{-4}$M, 3mg), HNO3 (0.02M) (stock solution in CH_3CN of 65% aqueous solution HNO_3) and substrate (0.5M) in acetonitrile (up to 2.5ml). The aliquots of the reaction solution were analysed by GC (the instrument Chromos-1000, fused silica capillary column FFAP/OV-101 20/80 w/w, 30 m × 0.2 mm × 0.3 μm; helium as a carrier gas). Attribution of peaks was made by comparison with chromatograms of authentic samples, the internal standards were nitromethane for kinetic tests). Usually samples were analyzed twice, i.e. before and after the addition of the excess of solid PPh_3 This method was developed and used previously.[51-52]

Alkyl hydroperoxides are transformed in the GC injector into a mixture of the corresponding ketone and alcohol. Due to this we quantitatively reduced the reaction samples with PPh_3 to obtain the corresponding alcohol. This method allows us to calculate the real concentrations not only of the hydroperoxide but of the alcohols and ketones present in the solution at a given moment.

Oxidation of Alcohol

The oxidation of alcohol was carried out similarly to the procedure for the oxidation of alkanes with the addition of triphenylphosphine.

References

S1 (a) B. Schowtka, C. Müller, H. Görls and M. Westerhausen, *Z. Anorg. Allg. Chem*. **2014**, *640*, 916; (b) K. Muller, Y. Sun, A. Heimermann, F. Menges, G. NiednerSchatteburg, C. van Wullen, W.R. Thiel. *Chem. Eur. J.* **2013**, *19*, 7825.

S2 T. G. G. Battye, L. Kontogiannis, O. Johnson, H. R. Powell, A. G. W. Leslie, *Acta Cryst.* **2011**, *D67*, 271-281.

S3 P. R. Evans, *Acta Cryst.* **2006**, *D62*, 72-82.

S4 Rigaku, *CrysAlisPro Software System, v. 1.171.41.106a*, Rigaku Oxford Diffraction, **2021**.

S5 A. L. Spek, *PLATON*, A Multipurpose Crystallographic Tool, Utrecht University, the Netherlands, **2015**.

S6 G. M. Sheldrick, *Acta Cryst.* **2015**, *C71*, 3-8.